The International Journal of Advanced Manufacturing Technology (2019) 101:913–926
https://doi.org/10.1007/s00170-018-2970-1

ORIGINAL ARTICLE

Relationship between mechanical properties and geometric parameters to limitation condition of springback based on springback–radius concept in V-die bending process

Daw-Kwei Leu [1]

Received: 12 September 2018 / Accepted: 30 October 2018 / Published online: 9 November 2018

Abstract
The determination of the accuracy of part geometry is based on the precise prediction of the springback–radius in sheet bending. Incorporating strength ratio, normal anisotropy, the strain-hardening exponent, and the geometric ratio, a simplified model is proposed to predict the springback–radius in V-die bending based on elementary bending theory. Experiments were conducted to validate the derived equation based on the proposed modeling for this radius. The calculation of springback–radius agrees closely with the experimental results, proving the reliability of the present model. To reduce springback and achieve the correct radius of bent parts in the sheet bending process, the effects of process parameters, including punch radius, material strength and sheet thickness, on springback–radius ratio (punch radius divided by the radius of bending after unloading) were experimentally examined to identify those that govern springback variations for a high-strength steel sheet. The manner in which the strength ratio (material constant divided by elastic constant), normal anisotropy, strain-hardening exponent, and geometric ratio (sheet thickness divided by punch diameter) affect springback–radius in the V-die bending process for high-strength steel sheet is theoretically examined. Finally, a relationship between mechanical properties and geometric parameters to limitation condition of springback based on springback–radius concept in V-die bending process is examined. The goal is to improve the accuracy of the springback–radius after unloading in the V-die bending process.

Keywords Sheet · Bending · Springback · Anisotropy · Hardening

1 Introduction

In manufacturing processes, structural stamping parts are typically fabricated in sheet metal bending processes. V-die bending is one of the most important sheet metal bending processes, which comprises two important sub-processes—air-bending and coining. The development of bending mechanics involves improving the following important practical techniques; the first is for predicting springback for bending die design, process programming and bending radius (or angle) control, and the second is for assessing the failure mechanism that is caused by the stretching of the outer surface at the bending point or bendability (which is occasionally defined as the minimum of the bending radius). The cause of the springback phenomenon is the elastic recovery after unloading, which refers to the recovery of the radius of curvature of a bent material fiber as the bending moment is removed in the unloading procedure. In process programming in bending, the essential die design, process control, and bent radius assessment are based on the precise prediction of springback.

Many researchers have sought to improve our understanding of the bending process. Gardiner [1] was the first to study the springback of metals and derived an equation for the springback–radius based on elementary theory. Datsko and Yang [2] studied the bendability of materials and identified a relationship between bendability and the material's tensile properties. Takenaka et al. [3] studied the relationships between material's tensile characteristics and bendability. They presented a method to measure the values of these characteristic. Cupka et al. [4] presented a new fine-bending technique based on the application of counter pressure. Kals and

✉ Daw-Kwei Leu
dkleu@tpcu.edu.tw

[1] Department of Mechanical Engineering, Taipei City University of Science and Technology, No. 2, Xueyuan Road, Beitou, Taipei 112, Taiwan, Republic of China

Veenstra [5] studied the critical bent radius in sheet bending. Ogawa et al. [6] developed an elastic–plastic finite element model to simulate accurately springback processes in sheet metal bending. Wang et al. [7] developed a mathematical model of the bending of sheet metal under plane strain conditions. Leu [8] proposed a simplified bending model to determining the minimum bending radius (or bendability) and angle of bending before and after bending (or springback) for anisotropic sheet metals. Leu [9] studied how the parameters of the V-die bending process affected the springback of sheet steel based on a finite-element analysis. Huang [10] studied the characteristics of coining process of V-die bending using elastic–plastic finite-element simulation and analysis. Recently, Leu [11] studied the reduction of springback when the coining force is applied in the V-die bending process. Bakhshi-Jooybari et al. [12] experimentally and theoretically studied the springback phenomenon in both U-bending and V-bending processes for CK67 anisotropic steel sheet. Narayanasamy and Padmanabhan [13] studied how to calculate the bend force in the air-bending process using response surface methodology. Yu [14] studied the variation of elastic modulus with plastic deformation and examined how the elastic modulus affects springback during plastic deformation. Ozturk et al. [15] found that heat reduces the springback of a titanium sheet. Chatti and Hermi [16] studied the characteristics of springback with nonlinear elastic recovery. Baseri et al. [17] developed a model of springback in a V-die bending process using a back-propagation algorithm with fuzzy learning. Chen and Jiang [18] studied the effect of grain size on the micro V-bending process for a very thin metal sheet. Lee et al. [19] studied the effect of the anisotropic hardening of sheet metal on springback in pre-strained U-drawing/bending. Jiang and Chen [20] studied the effect of grain size of metal on springback during micro tube-bending. Fu [21] studied the factors that control springback in air-bending by performing a numerical analysis in ABAQUS FEA software. Malikov et al. [22] experimentally and theoretically studied the characteristics of bending force in the air-bending of structured sheet metals. Song and Yu [23] studied the springback of a T-section beam by combining a finite-element method with a neural network technique. Recently, Leu [24] conducted pioneering work on the deviation of the bending point in symmetric V-die bending with asymmetric sheet length.

Most sheet metals are fabricated by rolling. The mechanical properties of sheet metal vary with rolling direction as a result of their either having a preferred crystallographic orientation or mechanical fibering. In this study, a model that incorporates both normal anisotropy and strain-hardening is presented, and their effects on predicted springback–radius are considered. High-strength steel (HSS) has the advantages of being stronger and cheaper than other conventional metals. HSS is widely used in the fabrication of automotive structural parts, especially to reduce weight and energy consumption in their manufacture. Weinmann and Shippell [25] studied the effect of geometric parameters, including those of both bending tool and the workpiece, on bending forces and springback in the V-die bending of a high-strength low-alloy steel sheet. Ramezani et al. [26] studied the springback behavior of high-strength steel sheets in the V-bending process using finite-element analysis and a Stribeck friction model. Fu and Mo [27] conducted numerical analysis of the characteristics of the incremental air-bending process for high-strength sheet metal. Ramezani and Mohd Ripin [28] studied the V-die bending process of aluminum alloy 6061-T4 sheets using a dry friction model that incorporated the strain-hardening exponent and the contact area ratio in ABAQUS/Standard software. Fu and Mo [29] studied the characteristics of springback in the air-bending of high-strength sheet metal using the GA–BPNN technique. Kardes Sever et al. [30] studied the effect of variation of the E-modulus on springback in V-bending and U-bending processes for advanced high-strength steel AHSS-DP 780 under plastic deformation. Recently, Leu [31] studied the deviation of the position of the bending point in the V-die bending process with asymmetric dies for high-strength steel sheets SPFC 440 and 590 of JIS G3135. Leu [32] studied the precise prediction of springback by considering the high-order (quadric) term of bending strain under nonlinear plastic deformation. While considerable progress has been made in improving the modeling of sheet bending, existing theories must be further developed to the practical applications of recent findings. The anisotropy of sheet metal, a mechanical property, must be considered to enable the more realistic modeling of sheet metal forming. Moreover, a relationship between mechanical properties and geometric parameters to limitation condition of springback is valuable to understand springback mechanism and improve springback reduction.

In bending, tool design and production scheduling usually account for a large part of the setup time owing to the occurrence of springback. A simple method for precisely computing springback–radius, which significantly reduces design time and programming setup time, is therefore very practically valuable. In this study, material characteristics, such as nonlinear strain-hardening and normal anisotropy, and tool geometry, including sheet thickness and punch radius, are incorporated into the model of pure bending under the plane strain condition. A simplified equation for computing springback–radius is developed based on the work of Leu [32], in which only the linear term in the circumferential strain of bending is considered. The proposed model differs from others as the bending radius after unloading (or springback–radius) is considered to obtain a more precise value of the springback to determine accurately the bent shape within the region of

nonlinear plastic-deformation. In this study, famous Gardiner's equation [1] is used to compare with the present model. Morrison's work [33] is adopted to connect Gardiner's work [1] to plastic deformation with the effects of K and n in order to easy compare Gardiner's work with the present model. A series of experiments is conducted herein to verify the presented model. In addition, two published experimental works, carried out by Lopez et al. [34] and Zhang et al. [35], are used to verify the present model. Finally, the limitation condition of springback, an inequality, based on springback–radius concept is discussed. The developed equation is a guideline for tool and product design.

2 Analysis

To explore the relationship between mechanical properties and geometric parameters to limitation condition of springback based on springback–radius concept in V-die bending process, a proper model of bending with springback–radius is first developed.

To reduce the complexity of modeling, the following assumptions are made. (1) The material is a rigid-plastic and strain-hardening material with Hill's plastic anisotropy. (2) The bending deformation is under plane strain conditions. (3) The Bauschinger effect and strain rate are negligible.

The normal anisotropic value, which is a mechanical property of sheet metal material, is generally defined as

$$R = \frac{R_0 + 2R_{45} + R_{90}}{4} \tag{1}$$

where R_0, R_{45}, and R_{90} are the anisotropic values that are measured at 0, 45, and 90° of rolling direction.

The strain-hardening behavior of the sheet is expressed as

$$\sigma_e = K\varepsilon_p^n \tag{2}$$

where σ_e is the effective stress, ε_p is the effective strain, and K is a material constant (or strength coefficient). The power-law equation can be obtained from a simple tensile test.

Figure 1 shows a schematic diagram of the V-die bending process, and Fig. 2 shows a pure bending model, drawing on the work of Leu and Zhuang [32]. They are used to develop the springback model of V-die bending.

2.1 Pure bending moment M

From Fig. 2, the applied pure bending moment under the plane strain condition, based on the elementary bending theory, is as follows.

$$M = 2b\int_0^{\frac{t}{2}} \sigma_\theta y dy \tag{3}$$

where σ_θ is the circumferential stress

$$\sigma_\theta = \frac{1+R}{\sqrt{1+2R}}\sigma_e \text{ and } \varepsilon_\theta = \frac{\sqrt{1+2R}}{1+R}\varepsilon_p \tag{4}$$

obeying Hill's theory of plastic anisotropy; ε_θ is the circumferential strain, and R is the normal anisotropy. Under the plastic deformation, the circumferential strain ε_θ can be expressed as

$$\varepsilon_\theta = \ln\left[\frac{\rho + y}{\rho}\right] \tag{5}$$

Neglecting the quadric term in the series, representation of the natural logarithm function enables the circumferential strain to be reduced to a linear term.

$$\varepsilon_\theta = \ln\left(1 + \frac{y}{\rho}\right) \approx \left[\frac{y}{\rho}\right] \tag{6}$$

Consideration of the linear term yields the circumferential stress σ_θ as

$$\begin{aligned}\sigma_\theta = \frac{1+R}{\sqrt{1+2R}}\sigma_e = \frac{1+R}{\sqrt{1+2R}}K\varepsilon_p^n = \frac{1+R}{\sqrt{1+2R}}K\left(\frac{1+R}{\sqrt{1+2R}}\varepsilon_\theta\right)^n \\ = K\left(\frac{1+R}{\sqrt{1+2R}}\right)^{1+n}\varepsilon_\theta^n\end{aligned} \tag{7}$$

Substituting Eq. (7) into Eq. (3) yields the applied bending moment of pure bending as

$$M = \frac{K}{4}\frac{bt^2}{(1+n)}\left(\frac{1+R}{\sqrt{1+2R}}\right)^{1+n}\left(\frac{t}{2\rho}\right)^n \tag{8}$$

Equation (8) gives the applied bending moment, which is a function of tool geometry and material properties, as derived by Leu [8].

2.2 Springback–radius ratio R_0/R_f

Springback is caused by the elastic recovery of materials upon unloading. The precise determination of springback is critical to determining the accuracy of part geometry. The unloading moment ΔM is assumed to have the same magnitude as the applied bending moment M, but the opposite sign, $\Delta M = -M$. The elastic deformation is given by

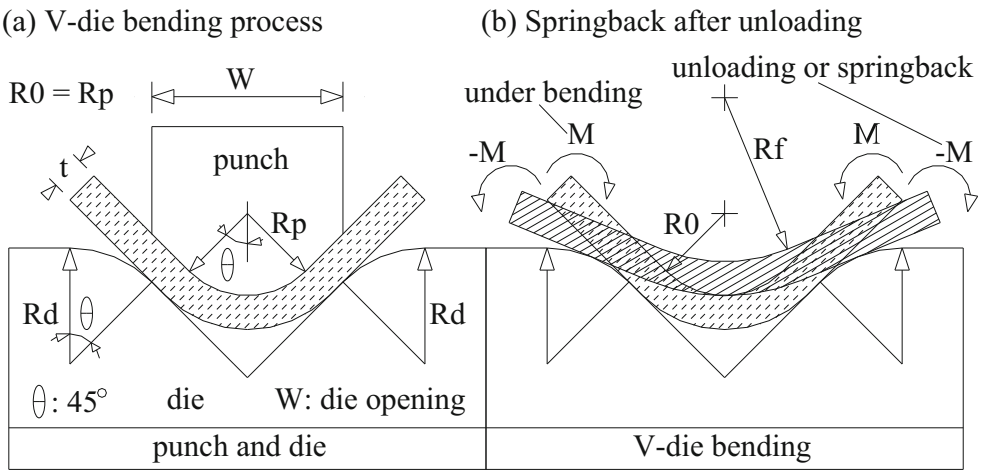

Fig. 1 **a** V-die bending process **b** Springback after unloading

$$\Delta\sigma_\theta = -\frac{My}{I} = E'\Delta\varepsilon_\theta \tag{9}$$

where

$$E' = \frac{E}{(1-\nu^2)} \tag{10}$$

Under the plane strain condition

$$\Delta\varepsilon_\theta = \frac{\Delta\sigma_\theta}{E'} = -\frac{My}{E'I} \tag{11}$$

and

$$\Delta\varepsilon_\theta = y\left(\frac{1}{\rho^*}-\frac{1}{\rho}\right) \tag{12}$$

From Eqs. (11) and (12), the following relationship is obtained.

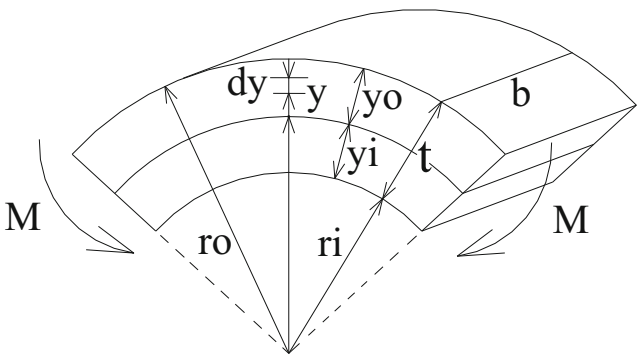

Fig. 2 Pure bending model [32] in which $r_i = R_0 = R_p$ and $r_o = r_i + t$

$$\frac{1}{\rho^*} = \frac{1}{\rho}-\frac{M}{E'I} \tag{13}$$

where ρ and ρ^* are the radii of the neutral axes before and after unloading, respectively.

Under elastic unloading, according to elementary bending theory, the unloading moment ΔM is

$$\Delta M = -M = \frac{bEt^3}{12(1-\nu^2)}\left(\frac{1}{\rho}-\frac{1}{\rho^*}\right) \tag{14}$$

where $(1-\upsilon^2)\approx 1$ or $E\approx E'$ is assumed. Substituting Eq. (8) into the above equation yields springback–radius ratio, defined as ρ/ρ^*, as

$$\frac{\rho}{\rho^*} = 1-\frac{3}{2}\frac{K}{E}\frac{1}{(1+n)}\left(\frac{1+R}{\sqrt{1+2R}}\right)^{1+n}\left(\frac{t}{2\rho}\right)^{n-1} \tag{15}$$

The terms R_0 and R_f are punch radius and bending radius after unloading, respectively, and $R_0\approx\rho$ and $R_f\approx\rho^*$ are assumed. Hence, Eq. (13) can be rewritten as

$$\frac{R_0}{R_f} = 1-\frac{3}{2}\left(\frac{1}{1+n}\right)\left(\frac{K}{E}\right)\left(\frac{1+R}{\sqrt{1+2R}}\right)^{1+n}\left(\frac{t}{2R_0}\right)^{n-1} \tag{16}$$

Equation (16) gives the springback–radius ratio, which is a function of the material properties (strength ratio K/E, strain-hardening exponent n, and normal anisotropy R) and tool geometry (thickness ratio $t/2\rho$). As reliability and accuracy of the equation of springback–radius ratio was proved, the limitation condition of springback, a relationship between mechanical properties and geometric parameters, can be properly explored. Subsequently, the validation of equation and discussion of relationship are shown as follows.

3 Results and discussion

In the first view of Eq. (16), the springback–radius is simply proportional to the strength constant K and inversely proportional to the modulus of elasticity E below the elastic limit. The modulus of elasticity E, or stiffness, is an important mechanical property.

To explore the relationship to limitation condition of springback, the first work is to verify the developed model of bending with springback–radius using experiment. Experimental measurements and numerical predictions were made. Experiments were conducted on the springback–radius of bending with various values of the process parameters, including punch radius, sheet thickness and material strength. The experiments verified the efficiency of the developed model. A numerical simulation was also conducted to study the effects of some process parameters on the springback–radius of the V-die bending process, using Eq. (16). Then, a relationship between mechanical properties and geometric parameters to limitation condition of springback, an inequality, based on springback–radius concept is examined in the final discussion.

3.1 Verification of springback–radius R_f

3.1.1 Verification of springback–radius R_f using experiments

Experimental materials were obtained from China Steel Corporation and are listed in Table 1 [32]. Figures 1 and 3 display the schemes of die, punch head, and hydraulic test machine. Table 2 presents the detailed dimensions of the tools that were used in the experiments. WD-40 mineral oil, a lubricant, was used. Experiments were performed using a 300-kN hydraulic test machine, and optical equipment was used to measure the springback angle. Springback–radius after unloading is difficult to directly measure its value in test. Therefore, a relationship is used to calculate the radius after bending. The relationship is based on the assumption that the bent length under bending (punch radius × bending angle) equals the bent length after bending or unloading (springback–radius × springback angle) in middle line of sheet thickness. First, three or two closer experimental data, springback angle after bending, obtained from five bending tests were employed to average the springback angle and then calculate the springback–radius using the mentioned relationship. The calculated springback–radius was truncated to three places of decimal in number.

The predicted values of springback–radius, calculated using Eq. (16), are compared with experimental values. The predicted values of springback–radius agree closely with the experimental values in Table 2, in which the range of error A, $R_f - R_f^e$, is from − 0.003 to − 0.034, indicating the reliability of the present method. Additionally, a numerical calculation of Gardiner's equation [1], a famous springback–radius equation used in many textbooks and reports, and the experimental data of two previously published experiments, Lopez et al. [34] and Zhang et al. [35] were adopted herein to objectively confirm the efficiency of the developed model for more various sheet materials.

3.1.2 Verification of springback–radius R_f using Gardiner's work [1]

To verify the efficiency of the present model, Eq. (17), derived by Gardiner [1] and used in many textbooks and reports, is compared with Eq. (16).

$$\frac{R_0}{R_f} = 4\left(\frac{R_0 Y}{Et}\right)^3 - 3\left(\frac{R_0 Y}{Et}\right) + 1 \text{ and } \frac{R_0}{R_f} = \left[\left(\frac{R_0}{t}\right)\left(\frac{Y}{E}\right) + 1\right]\cdot\left[2\left(\frac{R_0}{t}\right)\left(\frac{Y}{E}\right) - 1\right]^2 \tag{17}$$

or

$$\frac{R_0}{R_f} = 4\left(\frac{1}{2}\frac{Y}{E}\frac{2R_0}{t}\right)^3 - 3\left(\frac{1}{2}\frac{Y}{E}\frac{2R_0}{t}\right) + 1 \tag{18}$$

where Y is the yield stress and the effect of plastic deformation (material strength or strain-hardening exponent) is not considered. According to Morrison [33], yield stress Y can be obtained from the intercept of the strain-hardening portion of the stress–strain curve and the elastic modulus line:

$$Y = \left(\frac{K}{E^n}\right)^{\frac{1}{1-n}} \tag{19}$$

Equation (18) can be rewritten as

$$\frac{R_0}{R_f} = 4\left[\frac{1}{2}\left(\frac{t}{2R_0}\right)^{-1}\left(\frac{K}{E}\right)^{\frac{1}{1-n}}\right]^3 - 3\left[\frac{1}{2}\left(\frac{t}{2R_0}\right)^{-1}\left(\frac{K}{E}\right)^{\frac{1}{1-n}}\right] + 1 \tag{20}$$

which is a modified form of Gardiner–Morrison's equation, which connects Gardiner's work to plastic deformation with the effects of K and n. Equation (20) includes the same parameters as Eq. (16), so a comparison can be easily made.

The predicted values of springback–radius that are calculated by the method herein (Eq. (16)) and the method of Gardiner–Morrison (Eq. (20)) are compared with the experimental measurements in Table 2. From the errors (error A in the present work and error B in Gardiner–Morrison's work), the springback–radius that is calculated herein agrees closely with the experimental results and substantially more closely

Table 1 Material properties of HSS sheet manufactured by China Steel Company [32]

JIS G3135	t (mm)	E (GPa)	ν	σ_y (MPa)	$\sigma_e = K\varepsilon_p^n$ (MPa)
SPFC 440	1.4	205	0.3	285.9	$\sigma_e = 745.9\varepsilon_p^{0.201}$
SPFC 440	1.8	205	0.3	313.9	$\sigma_e = 739.9\varepsilon_p^{0.201}$
SPFC 590	1.8	205	0.3	287.8	$\sigma_e = 1161.6\varepsilon_p^{0.257}$

than that calculated using Gardiner–Morrison's method in cases with a large bend radius. However, both methods yield small errors (error A and error B) for a small bend radius. The small difference between these two calculated values of springback–radius demonstrates the reliability of the present method and that the presented model is better than the Gardiner–Morrison model for predicting the springback–radius of a high-strength steel sheet.

3.1.3 Verification of springback–radius R_f using Lopez-Castro's work [34]

To enable the practical application of the presented model, a published experiment that was performed by Lopez-Castro et al. [34] was repeated herein to confirm Eq. (16). Table 3 presents the mechanical properties of bright mild steel sheets EN-3B and CR-4, which were used in the experiments of Lopez-Castro et al. [34]. The springback–radius ratios, calculated using Eq. (16), are compared with the experimental measurements that were made by Lopez-Castro et al. [34] and presented in Fig. 4. The springback–radius ratio that is calculated herein using Eq. (16) agrees closely with the experimental data of Lopez-Castro. However, in the case of material CR-4, a clear difference exists, perhaps as a result of the neglect of the anisotropic property or the inhomogeneous properties of the sheet metal in the calculation (in which R is assumed to be unity).

Beyond the comparison between the springback–radius ratio obtained using Eq. (16) and that obtained experimentally by Lopez-Castro et al. [34], the accuracy of Gardiner's prediction is studied because Gardiner's work (Eq. (18)) provided the yield stress of experimental materials. Figure 5 compares the springback–radius ratio obtained using Eq. (16) with that obtained by Gardiner's equation based on the experiment that was performed by Lopez-Castro et al. [34] for two bright mild steel sheet materials, EN-3B and CR-4. The springback–radius ratio that is calculated by the present work and that obtained using Gardiner's equation both agree closely with the experimental value obtained by Lopez-Castro [34].

Figure 6 compares the springback–radius ratio obtained using Gardiner's work (Eq. (18)) with that obtained using Gardiner–Morrison's work (Eq. (20)) based on the experimental results of Lopez-Castro et al. [34] for two bright mild steel

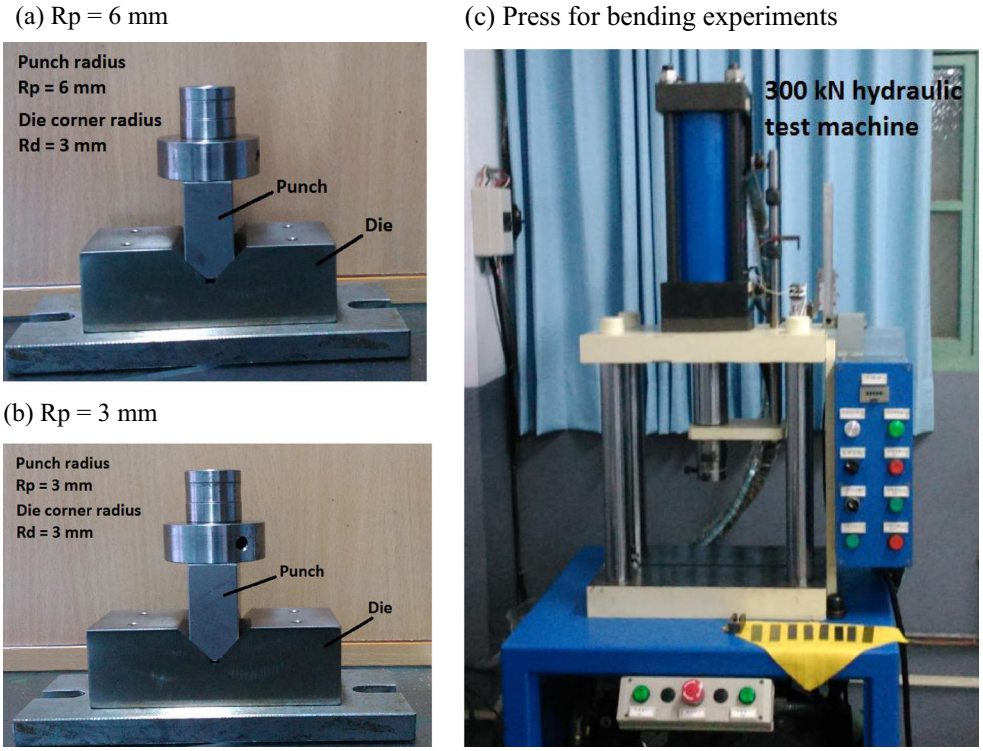

Fig. 3 Experimental tools for V-die bending, W = 25 mm and Rd = 3 mm taken from [32]. **a** Rp = 6 mm. **b** Rp = 3 mm. **c** Press for bending experiments

Table 2 Tool dimensions and experimental results concerning V-die bending

	Thickness t (mm)	Calculation R_f (mm)	Calculation R_f^* (mm)	Experiment R_f^e (mm)	Error A $R_f - R_f^e$	Error B $R_f^* - R_f^e$
$R_P = 6$ mm						
$R_d = 3$ mm						
SPFC 440	1.4	6.180	6.378	6.183	− 0.003	0.195
SPFC 440	1.8	6.150	6.284	6.155	− 0.005	0.129
SPFC 590	1.8	6.206	6.495	6.231	− 0.025	0.264
$R_P = 3$ mm						
$R_d = 3$ mm						
SPFC 440	1.4	3.052	3.092	3.077	− 0.025	0.015
SPFC 440	1.8	3.043	3.069	3.076	− 0.024	− 0.007
SPFC 590	1.8	3.061	3.119	3.095	− 0.034	0.024

$W = 25$ mm in Fig. 1; lubricant: WD-40 mineral oil and $R = 1$; R_f calculated using Eq. (16); R_f^* calculated using Eq. (20), taken from Gardiner–Morrison's work

sheet materials, EN-3B and CR-4. The prediction made using Gardiner's work is more accurate than that made using Gardiner–Morrison's work, indicating that Morrison's model seems not suitable for determining the hardening effect of plastic deformation in Eq. (19).

Finally, Fig. 7 compares the springback–radius ratio obtained using Gardiner's work with that obtained using Lopez-Castro's work (Eq. (21) shown as follows) based on the experiment of Lopez-Castro et al. [34]. However, the work of Lopez-Castro seems unsuitable for predicting the springback–radius ratio for sheet metal CR-4. A negative springback–radius ratio ($R_0/R_f = -2.3$) was calculated using the following Eq. (21), shown in Fig. 7, inconsistent with the actual limitation conditions of springback, $R_0/R_f > 0$. Lopez-Castro's equation [34] for the springback–radius ratio is as follows.

$$\frac{R_0}{R_f} = \frac{24K_E R_h^3}{n+2}\left(\varepsilon_t^{n+2} - h_R^{n+2}\right) + 4(R_h Y_E)^3 - 12R_h^3 Y_E \varepsilon_t^2 + 1$$

or

$$\frac{R_0}{R_f} = \frac{3}{n+2}\left(\frac{2R_0}{t}\right)^3\left(\frac{K}{E}\right)\left(\varepsilon_t^{n+2} - \left(\frac{t}{2R_0}\right)^{n+2}\right) + \frac{1}{2}\left(\frac{2R_0}{t}\right)^3\left(\frac{K}{E}\right)^{\frac{3}{1-n}} - \frac{3}{2}\left(\frac{2R_0}{t}\right)^3\left(\frac{K}{E}\right)^{\frac{1}{1-n}}\varepsilon_t^2 + 1 \quad (21)$$

However, Gardiner's equation, Eq. (17), is a special case of Lopez-Castro's equation, Eq. (21), when $n = 0$, $K = Y$, and $\varepsilon_t = Y/E$.

3.1.4 Verification of springback–radius R_f using Zhang's work [35]

To extend the application of the present model, the experiment of Zhang et al. [35] is used to verify the model herein and compare it with that of Gardiner's equation. Table 4 presents the materials that were used by Zhang et al. [35]—HSS and Al 6111-T4 sheet metals. The values of springback–radius that were calculated using the present model (Eq. (16)) are compared with the experimental values that were measured by Zhang et al. [35] in Table 5. Clearly Zhang's model best fits (smallest difference between calculation and experiment, error 2) the experimental values. Then, the errors (error 1) indicate that the springback–radius that was calculated herein (Leu's work) agrees closely with the experimental results and is better than that obtained using Gardiner's work (error 3) as presented in Figs. 8 and 9. The small difference between the calculated and experimental values of springback–radius indicates the reliability of the method herein, and the fact that the present model is better than that of Gardiner [1] for calculating the values of springback–radius of aluminum and high-strength steel sheet metals.

A comparison of present model to other models in predicting springback–radius for various sheet metals is made to find out the accuracy of each model as shown in Table 6.

1. First column of Table 6 for steel sheet SPFC (Cold-reduced high strength steel sheet): The accuracy of present model is better than Gardiner–Morrison's equation in the case of large punch radius (Rp = 6 mm) and small die corner radius (Rd = 3 mm). On the other hand, the accuracy of Gardiner–Morrison's

Table 3 Material properties of sheet metal EN-3B and CR-4 used by Lopez-Castro et al. [34]

Material	t (mm)	E (GPa)	Y (MPa)	$\sigma_e = K\varepsilon_p^n$ (MPa)
CR-4	1.0	211.0	250.0	$\sigma_e = 413.0\varepsilon_p^{0.1282}$
EN-3B	3.0	190.0	450.0	$\sigma_e = 708.0\varepsilon_p^{0.0764}$
EN-3B	5.0	195.0	320.0	$\sigma_e = 588.0\varepsilon_p^{0.1530}$

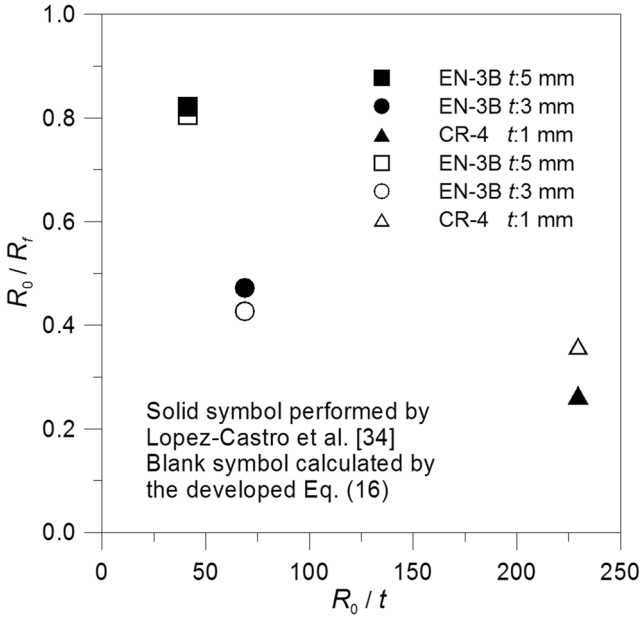

Fig. 4 Comparison of springback–radius ratio obtained using present model Eq. (16) and the experimental value obtained by Lopez-Castro et al. [34] with two bright mild steel sheet materials, EN-3B and CR-4

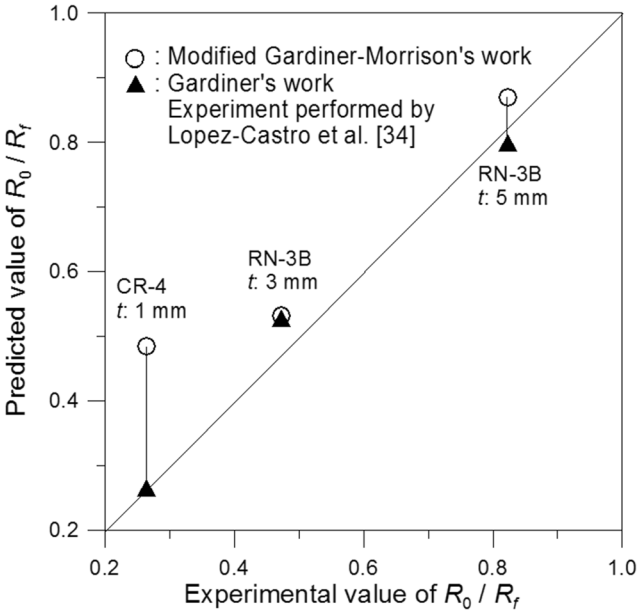

Fig. 6 Comparison of springback–radius ratio obtained using Gardiner's work [1] with that obtained using Gardiner–Morrison's work (Eq. (20)), based on experiment conducted by Lopez-Castro et al. [34]

equation is better than the present model in the case of small punch radius (Rp = 3 mm) and small die corner radius. Punch radius significantly affects springback behavior.

2. Second column of Table 6 for steel sheets CR-4 and EN-3B (Bright mild steel sheet) [34]: The Lopez-Castro's model failed to predict springback–radius in the case of CR-4 because a negative springback–radius was obtained. The accuracy of Gardiner's equation is better than the others in the case of CR-4. On the other hand, the accuracy of the present model is better than the others in the case of EN-3B. The calculated value of the case CR-4 seems varied and unpredictable, which calculated value may be an exact solution (0.0% error by Gardiner [1]) or too large (83.16% error by Gardiner–Morrison's equation, Eq. (20)) or fail to predict (a negative value by Lopez-Castro's model [34]).

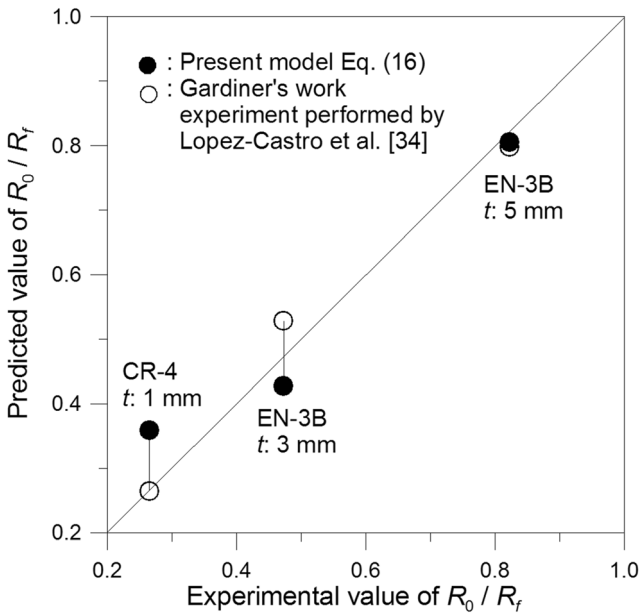

Fig. 5 Comparison of springback–radius ratio obtained using present model Eq. (16) and that obtained using Gardiner's work [1], based on experiment conducted by Lopez-Castro et al. [34]

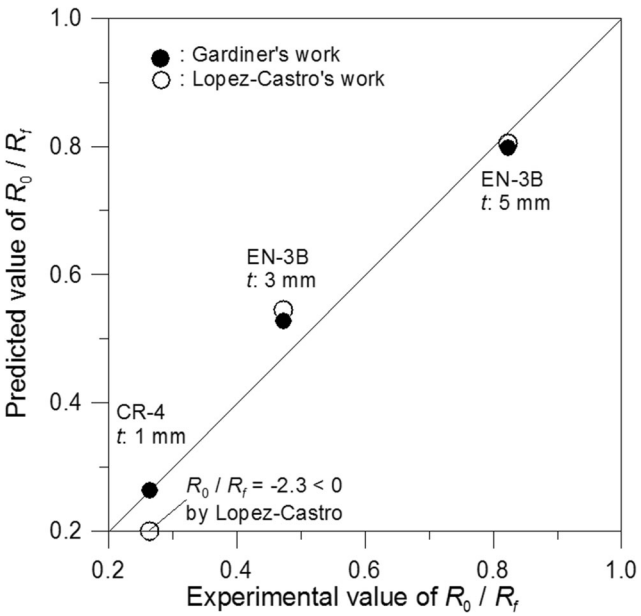

Fig. 7 Comparison of springback–radius ratio obtained using Gardiner's work [1] with that obtained using Lopez-Castro's work [34], based on experiment conducted by Lopez-Castro et al. [34]

Table 4 Material properties of sheet metal HSS and 6111-T4 used by Zhang et al. [35]

	ν	E (GPa)	R	$\sigma_e = K\varepsilon_p^n$ (MPa)
HSS				
0	0.3	217.50	1.520	$\sigma_e = 645.24\varepsilon_p^{0.25177}$
45	0.3	220.03	2.096	$\sigma_e = 632.11\varepsilon_p^{0.25332}$
90	0.3	230.56	2.375	$\sigma_e = 615.09\varepsilon_p^{0.25409}$
6111-T4				
0	0.346	70.5	0.894	$\sigma_e = 550.4\varepsilon_p^{0.223}$
45	0.333	71.4	0.611	$\sigma_e = 534.5\varepsilon_p^{0.224}$
90	0.346	69.6	0.660	$\sigma_e = 533.5\varepsilon_p^{0.231}$

$t = 1$ mm and $Rn = 24$ mm for HSS and 611-T4 sheet metal.

3. Third column of Table 6 for sheet metals HSS and 6111-T4 (high strength steel and aluminum alloy sheets) [35]: The accuracy of Zhang's model is better than the present model for steel sheet HSS. Then, the accuracy of the present model is better than Gardiner's model for steel sheet HSS. On the other hand, the accuracy of the present model is close to Zhang's model in the case of 6111-T4. Of all the three models, the accuracy of Gardiner's equation seems the worst for aluminum alloy 6111-T4.

In general, the present model shows its reliability and efficiency in predicting springback–radius of steel metal sheet even though it is not the best model of all these models.

3.2 Effects of material properties and tool geometry on springback–radius

3.2.1 Effects of material properties and tool geometry on springback–radius based on experimental results

Figure 10a–c plots the experimentally determined effects of punch radius, sheet thickness, and material strength on springback–radius. Figure 10a indicates that the springback–radius slightly decreases as the sheet thickness increases for material SPFC 440, with a punch radius Rp = 6 and 3 mm. This effect arises from the fact that increasing the thickness reduces the elastic recovery of a sheet by increasing the bulk deformation. However, the increase in the springback–radius is limited for Rp = 3 mm. The punch radius apparently has an important role in springback. Figure 10b indicates that springback–radius increases with material strength (SPFC 590 > SPFC 440) at $t = 1.8$ mm and Rp = 6 and 3 mm. This effect arises from the fact that reducing material strength reduces the elastic recovery by reducing the rigidity of the material. However, the springback–radius at Rp = 6 mm is only slightly larger than that at Rp = 3 mm, indicating that the punch radius has an important role in springback. Figure 10c indicates that the springback–radius increases with the

Table 5 Experimental results concerning V-die bending performed by Zhang et al. [35]

	A (mm)	B (mm)	C (mm)	D (mm)	Error 1 B-A	Error 2 C-A	Error 3 D-A
HSS							
0°	26.48	26.24	26.61	25.73	−0.24	0.13	−0.75
45°	26.83	26.40	26.90	25.84	−0.43	0.07	−0.99
90°	26.72	26.31	26.80	25.71	−0.41	0.08	−1.01
6111-T4							
0°	30.76	31.01	30.73	29.89	0.25	−0.03	−0.57
45°	30.10	30.13	29.96	29.22	0.03	−0.14	−0.88
90°	29.98	30.14	29.92	29.21	0.16	−0.06	−0.77

Experimental value of R_n' (= R_f) based on $R_n\theta_1 = R_n'\theta_1'$, A: experimental data; B: the present model (Leu's work); C: Zhang's equation; D: Gardiner's equation

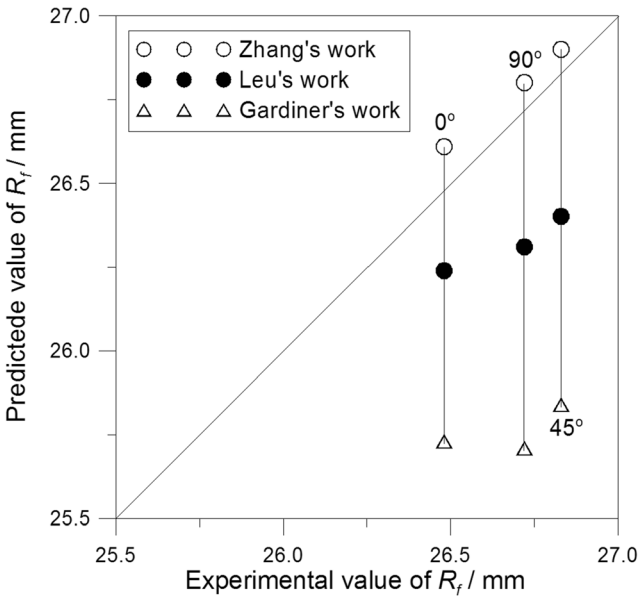

Fig. 8 Comparison of springback–radius in Gardiner's work [1], Zhang's work [35], and Leu's work (Eq. (20)) for sheet metal HSS, based on experiment conducted by Zhang et al. [35]

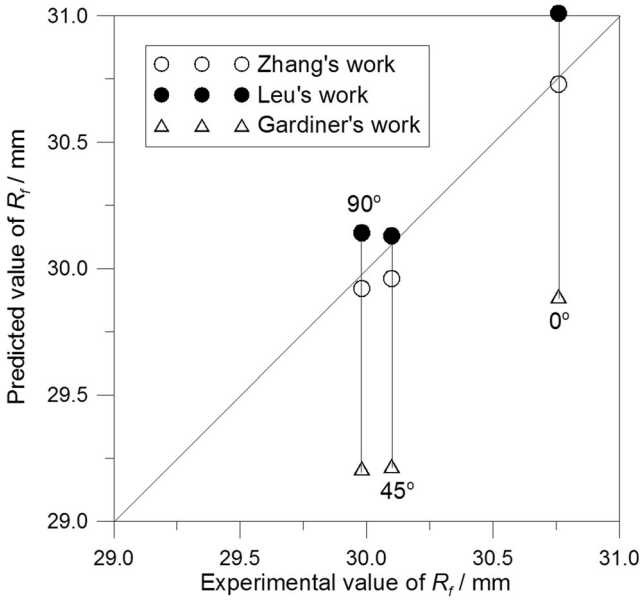

Fig. 9 Comparison of springback–radius in Gardiner's work [1], Zhang's work [35], and Leu's work (Eq. (20)) for sheet metal 6611T4, based on experiment conducted by Zhang et al. [35]

punch radius for SPFC 440 and 590, $t = 1.4$ and 1.8 mm. This effect arises from the fact that reducing the punch radius reduces the elastic recovery by concentrating the plastic zone in the bent part of workpiece. The increase in the springback–radius of SPFC 590 at $t = 1.8$ mm is larger than that of SPFC 440. From Fig. 10a–c, increasing the sheet thickness, reducing the material strength, and reducing the punch radius effectively reduce the increase in the springback–radius (or springback) in the V-die bending process.

3.2.2 Effects of material properties and process geometry on springback–radius ratio R_0/R_f in theoretical manner

In addition to experiments, numerical simulations, based on the present model (Eq. (16)) and Gardiner–Morrison's work (Eq. (20)), were performed to study the effect of the process parameters, strength ratio K/E, strain-hardening exponent n, geometric ratio $t/2R_0$, and normal anisotropy R, on the springback–radius ratio R_0/R_f in the V-die bending process, as presented in Figs. 11 and 12.

Figures 11a–c compares the effects of process parameters on springback–radius ratio in this work and in Gardiner–Morrison's work. The relationship is similar in both cases, but the rates of change with process parameters differ. The results of Gardiner–Morrison are always greater than those obtained using the present model, Eq. (16). Figure 11 supports the following conclusions. (i) The springback–radius ratio decreases almost linearly as the strength ratio increases and the rate of decrease increases with n and $t/2R_0$; (ii) the springback–radius ratio increases with the strain-hardening exponent or geometric ratio. For large n, R, and $t/2R_0$ (Fig. 11a), reducing K/E slightly increases the springback–radius ratio for the rate reduced in the present model. Generally, the effect of K/E on the springback–radius ratio is greater for smaller values of n, R, and $t/2R_0$ in the present model. On the other hand, the springback–radius ratio remains constant under increasing n and $t/2R_0$ (Fig. 11a) or increasing K/E and n (Fig. 11c). For large values of n, the effects of K/E and $t/2R_0$ on springback–radius ratio are very limited (Fig. 11b) in the Gardiner–Morrison's model.

The effect of normal anisotropy R was ignored by Gardiner's work [1] and Lopez-Castro's work [34].

Table 6 Errors of springback–radius in percentage between experiment and prediction for different models

Error % (Cal-Exp) / Exp × 100%	Present experiment				Lopez-Castro's experiment [34]			Zhang's experiment [35]		
		SPFC 440 $t = 1.4$	SPFC 440 $t = 1.8$	SPFC 590 $t = 1.8$	CR4 $t = 1$	EN3B $t = 3$	EN3B $t = 5$		HSS	6111-T4
Leu's model, Eq. (16)	A	− 0.048	− 0.081	− 0.40	35.93	− 0.50	− 2.01	0^0	− 0.91	0.81
								45^0	− 1.60	0.09
	B	− 0.81	− 0.78	− 1.09				90^0	− 1.53	0.53
Gardiner's model [1] or Eq. (17)	Non				0.00	11.90	− 2.90	0^0	− 2.83	− 1.85
								45^0	− 3.68	− 2.92
								90^0	− 3.77	− 2.56
Gardiner–Morrison, Eq. (20)	A	3.15	2.09	4.23	83.16	12.74	5.76	Non		
	B	− 0.48	− 0.22	− 0.77						
Lopez-Castro's model [34]	Non				Fail	15.45	− 2.16	Non		
Zhang's model [35]	Non				Non			0^0	0.49	− 0.09
								45^0	0.26	− 0.46
								90^0	0.29	− 0.20

A: Rp = 6 mm, Rd = 3 mm; B: Rp = 3 mm, Rd = 3 mm; (Cal-Exp) / Exp = (prediction-experiment)/experiment × 100%

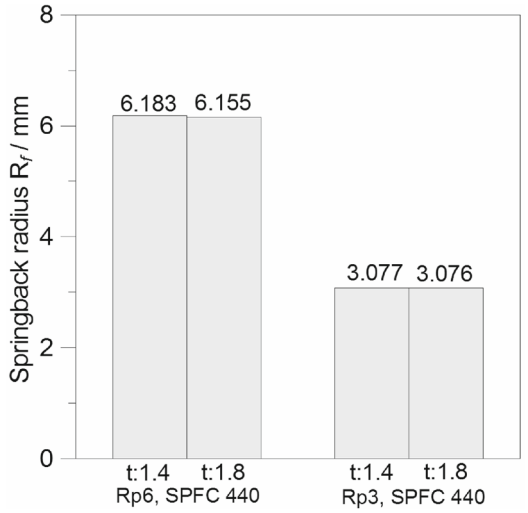

(a)

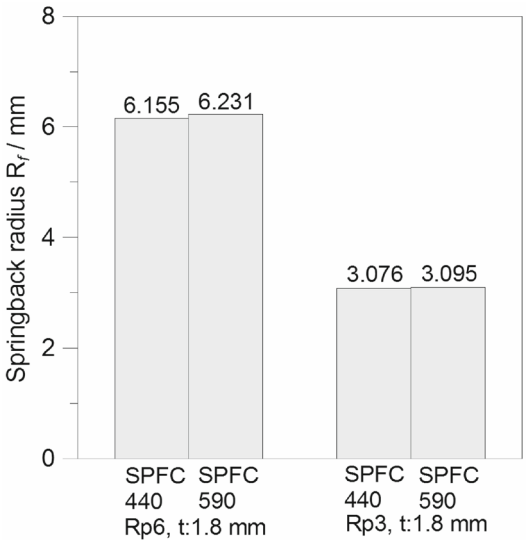

(b)

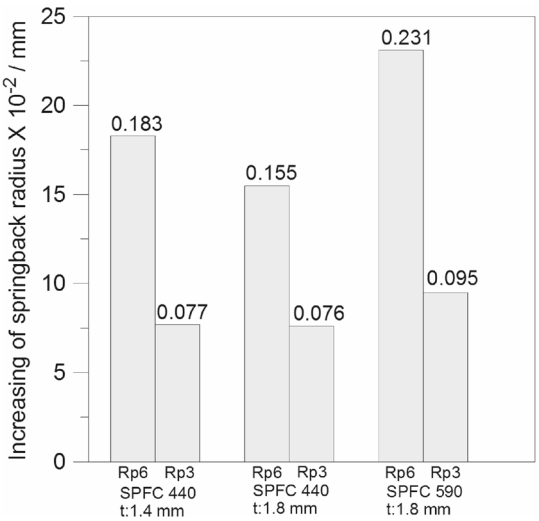

(c)

◀ **Fig. 10** **a** Effect of thickness on springback–radius for various punch radii. **b** Effect of material strength on springback–radius for various punch radii. **c** Effect of punch radius on springback–radius for different thicknesses and material strengths

Parameter normal anisotropy R is an individual characteristic of mechanical property, which included in the present model is the feature of this study. Figure 12 presents the effect of normal anisotropic parameter on springback–radius ratio for different values of strength ratio, strain-hardening exponent and geometric ratio, based on the present model. The effect of normal anisotropy R on the springback–radius ratio is the same as that of K/E, closely linear relationship that the springback–radius ratio decreases almost linearly as normal anisotropy increases.

3.3 A relationship between mechanical properties and geometric parameters to limitation condition of springback based on springback–radius concept

The reliability and efficiency of the present model of bending used to predict springback–radius have been proved shown in Sects. 3.1 to 3.2. Subsequently, the constraining condition on springback, $0 < R_0/R_f < 1$, arose for more understanding the springback behavior and more effectively improving the springback reduction. However, this topic is important but seldom be mentioned at present.

Gardiner's work [1] is very famous and common use in the springback–radius prediction. Therefore, a further analysis concerning the critical condition (or limitation condition) in Gardiner's work, Eq. (17), is as follows. With respect to the constraining condition on springback, $0 < R_0/R_f < 1$, the condition of $0 < R_0/R_f$ always holds in Eq. (17), and a relation that is based on the condition $R_0/R_f < 1$ can be obtained as follows.

$$\left(\frac{Y}{E}\right)\left(\frac{R_0}{t}\right) < \frac{\sqrt{3}}{2} \text{ or } \left(\frac{Y}{\sqrt{3}E}\right) < \left(\frac{t}{2R_0}\right) \tag{22}$$

where $(Y/E)(R_0/t) = 1/2$ is no permitted since $R_0/R_f \neq 0$ according to Eq. (17). Equation (22) is based on Gardiner's equation and shows an interesting relationship between material characteristics (Y and E) and geometric parameters (t and R_0) under the constraining condition (limitation condition) on springback, $0 < R_0/R_f < 1$. The free springback is under the condition of $R_0/R_f = 1$, and a relationship between material characteristics (Y and E) and geometric parameters (t and R_0) is obtained as.

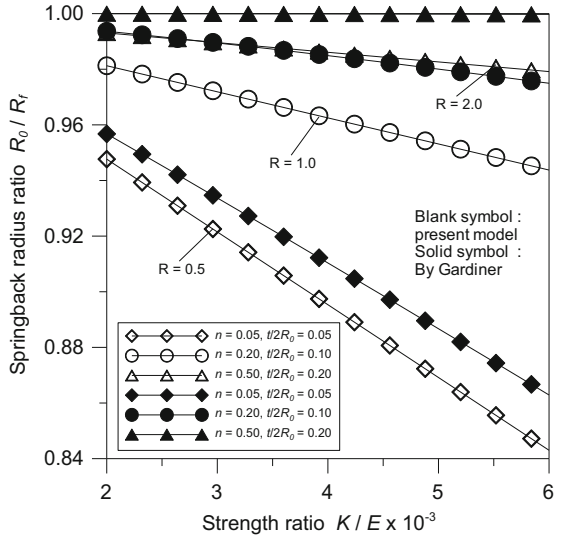

(a)

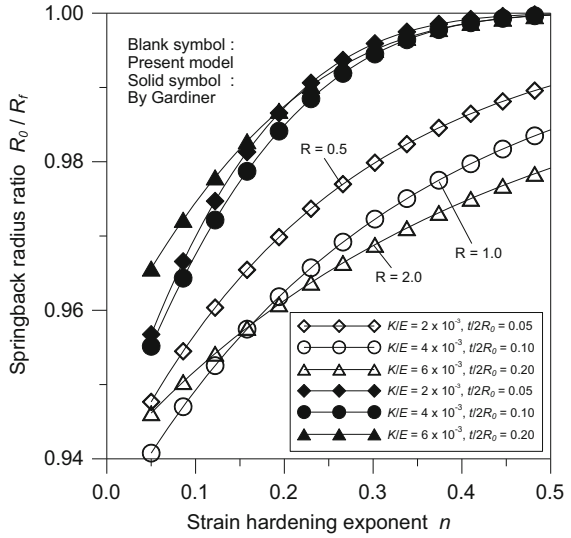

(b)

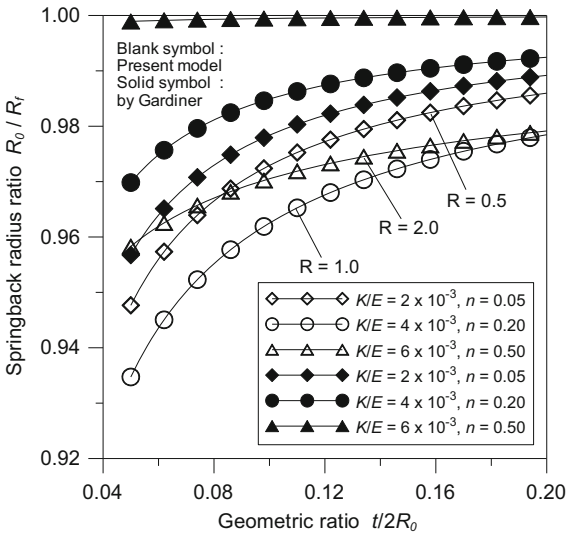

(c)

◀ **Fig. 11** **a** Comparison of effects of strength ratio on springback–radius ratio for different strain-hardening exponents and geometric ratios; blank symbol indicates present model, and solid symbol indicates model of Gardiner–Morrison. **b** Comparison of effects of strain-hardening exponent on springback–radius ratio for different strength ratios and geometric ratios; blank symbol indicates present model, and solid symbol indicates model of Gardiner–Morrison. **c** Comparison of effects of geometric ratio on springback–radius ratio for different strength ratios and strain-hardening exponents; blank symbol indicates present model, and solid symbol indicates model of Gardiner–Morrison's work

$$\left(\frac{Y}{\sqrt{3}E}\right) = \left(\frac{t}{2R_0}\right) \tag{23}$$

From Gardiner–Morrison's equation, a similar relation to Eq. (23) that pertains the constraining condition on springback is

$$\frac{1}{\sqrt{3}}\left(\frac{K}{E}\right)^{\frac{1}{1-n}} < \left(\frac{t}{2R_0}\right) \tag{24}$$

Equation (24) that is based on Gardiner–Morrison's equation shows an interesting relationship between material characteristics (K, E and n) and geometric parameters (t and R_0). Under the condition of $R_0/R_f = 1$, a relationship between material characteristics (K, E, and n) and geometric parameters (t and R_0) to free springback is obtained as

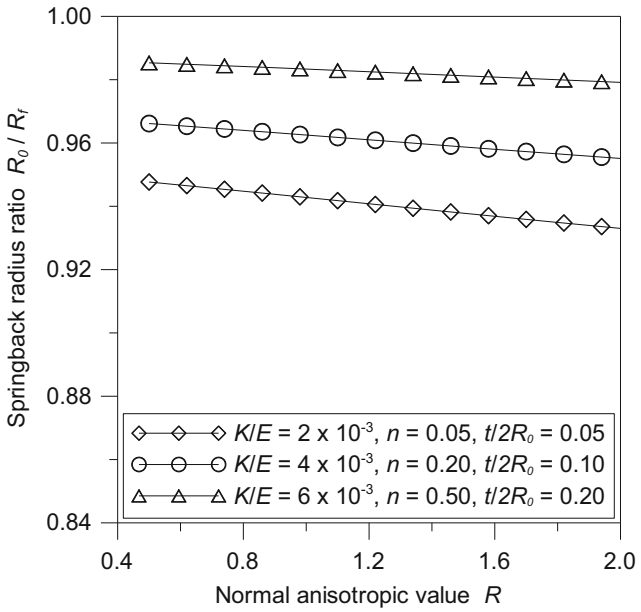

Fig. 12 Effect of normal anisotropic parameter on springback–radius ratio for different values of strength ratio, strain-hardening exponent and geometric ratio, based on the present model

$$\frac{1}{\sqrt{3}}\left(\frac{K}{E}\right)^{\frac{1}{1-n}}=\left(\frac{t}{2R_0}\right) \tag{25}$$

Under the constraining condition (limitation condition) on springback, $0<R_0/R_f<1$, the presented model, Eq. (16), yields a relationship as follows.

$$\left(\frac{K}{E}\right)^{\frac{1}{1-n}}\left[\frac{3}{2}\left(\frac{1}{1+n}\right)\right]^{\frac{1}{1-n}}\left(\frac{1+R}{\sqrt{1+2R}}\right)^{\frac{1+n}{1-n}}<\left(\frac{t}{2R_0}\right) \tag{26}$$

Equation (26) is similar with Eqs. (23) and (24), in which unit is dimensionless and shows a more complicated and general relationship between material characteristics (K, E, R, and n) and geometric parameters (t and R_0). However, the relationship between material characteristics (K, E, R and n) and geometric parameters (t and R_0) to free springback, satisfying the condition of $R_0/R_f=1$, is obtained as

$$\left(\frac{K}{E}\right)^{\frac{1}{1-n}}\left[\frac{3}{2}\left(\frac{1}{1+n}\right)\right]^{\frac{1}{1-n}}\left(\frac{1+R}{\sqrt{1+2R}}\right)^{\frac{1+n}{1-n}}=\left(\frac{t}{2R_0}\right) \tag{27}$$

The constraining condition (limitation condition) on springback is defined as $0<R_0/R_f<1$. However, a negative springback–radius ratio ($R_0/R_f=-2.3<0$) was calculated using Lopez-Castro's work [34] (Eq. (21)) shown in Fig. 7 (the case of sheet metal CR-4), which is inconsistent with the actual conditions of springback, $R_0/R_f>0$. Lopez-Castro's work seems unsuitable for analyzing the constraining condition of springback, but the other constraining conditions of springback, i.e., analyzed that

$$\varepsilon_t^{n+2}+\frac{n+2}{6}\left(\frac{K}{E}\right)^{\frac{2+n}{1-n}}-\frac{n+2}{2}\left(\frac{K}{E}\right)^{\frac{n}{1-n}}\varepsilon_t^2<\left(\frac{t}{2R_0}\right)^{n+2} \tag{28}$$

The above equation is a complicated relationship between material properties (K, E, n and ε_t) and process geometry (t and R_0), so further work is needed to clarify the contradiction of the condition of $R_0/R_f<0$. However, the relationship between material characteristics (K, E, n and ε_t) and geometric parameters (t and R_0) to free springback, satisfying the condition of $R_0/R_f=1$, is obtained as

$$\varepsilon_t^{n+2}+\frac{n+2}{6}\left(\frac{K}{E}\right)^{\frac{2+n}{1-n}}-\frac{n+2}{2}\left(\frac{K}{E}\right)^{\frac{n}{1-n}}\varepsilon_t^2=\left(\frac{t}{2R_0}\right)^{n+2} \tag{29}$$

Varied conditions of free springback, such as Eqs. (23), (25), (27), and (29), show that the relationship between mechanical properties and geometric parameters is restricted to a specific relation. Therefore, a more complete study is needed to clarify and distinguish the effects of process parameters on springback reducing for precisely shape control in bending process.

4 Conclusions

This work develops a simplified method, incorporating strength ratio K/E, geometric ratio $t/2R_0$, normal anisotropy R and strain-hardening exponent n, for estimating the springback–radius ratio in V-die bending, based on elementary bending theory and the pure bending model. A series of experiments are conducted to confirm the proposed model and to clarify the effects of punch radius, sheet thickness, and material strength on springback–radius. Using this simplified method, the relationship between mechanical properties and geometric parameters to limitation condition of springback, especially for the free springback condition, is examined. The following findings were obtained.

(1). A comparison between predicted and experimental values indicates agreement, indicating the reliability of the presented model. The model herein is more accurate than previously developed models for predicting springback of steel metal sheet, such as those of Gardiner [1] and Gardiner–Morrison (Eq. (20)).

(2). In the developed model, the springback–radius is simply proportional to the initial strain and inversely proportional to the modulus of elasticity within the elastic limit, owing to the linear elastic recovery.

(3). The experimental results demonstrate that increasing the sheet thickness, reducing the material strength and reducing the punch radius effectively reduce the springback–radius in the V-die bending process.

(4). Numerical simulations indicate that the springback–radius ratio increases as the normal anisotropy and the strength ratio increase or as the geometric ratio and strain-hardening exponent decrease. The effects of K/E and $t/2R_0$ are limited for large values of n. Generally, the effect of K/E exceeds those of small values of n, R, and $t/2R_0$.

(5). An interesting relationship (an inequality) between material characteristics (Y, K, E, R and n) and geometric parameters (t and R_0) under the constraining condition (limitation condition) of springback, $0<R_0/R_f<1$, is derived. Moreover, the free springback under the condition of $R_0/R_f=1$ is also discussed, and a relationship between material characteristics and geometric parameters for free springback is obtained. However, a more complete study to clarify and distinguish the effects of process parameters on the constraining condition of springback is needed for precisely shape control in bending process.

This work can be used as a process design guideline for reducing the springback of high-strength steel sheets in V-die bending.

Acknowledgments H. Y. Chou is appreciated for the help in the experiments.

Funding information The author would like to thank the Ministry of Science and Technology of the Republic of China, Taiwan, for financially supporting this research under Contract No. MOST 106-2221-E-149-001.

References

1. Gardiner FJ (1957) The springback of metals. ASME J Appl Mech 79:1–9
2. Datsko J, Yang CT (1960) Correlation of bendability of materials with their tensile properties. ASME J Eng Ind 82:309–314
3. Takenaka N, Tozawa Y, Suzuki K (1970) Material characteristic value for evaluation of bendability and methods for measuring these values. Ann CIRP 20:53–54
4. Cupka V, Nakagawa T, Tiyamoto H, Kudo H (1973) Fine bending with counter pressure. Ann CIRP 22:73–74
5. Kals JAG, V-dienstra PC (1974) On the critical radius in sheet bending. Ann CIRP 23:55–56
6. Ogawa H, Makinouchi A, Takizawa H, Mori N (1993) Development of an elasto-plastic FE code for accurate prediction of springback in sheet bending processes and its validation by experiments. In: Advanced Technology of Plasticity, Proceeding of the Fourth International Conference on Technology of Plasticity, pp 1641–1646
7. Wang C, Kinzel G, Altan T (1993) Mathematical modeling of plane-strain bending of sheet and plate. J Mater Process Technol 39:279–304
8. Leu DK (1997) A simplified approach for evaluation bendability and springback in plastic bending of anisotropic sheet metals. J Mater Process Technol 66:9–17
9. Leu DK (1998) Effects of process variables on V-die bending process of steel sheet. Int J Mech Sci 40(7):631–650
10. Huang YM (2007) Finite element analysis on the V-die coining bend process of steel metal. Int J Adv Manuf Technol 34:287–294
11. Leu DK, Hsieh CM (2008) The influence of coining force on spring-back reduction in V-die bending process. J Mater Process Technol 196:230–235
12. Bakhshi-Jooybari M, Rahmani B, Daeezadeh V, Gorji A (2009) The study of spring-back of CK67 steel sheet in V-die and U-die bending processes. Mater Des 30(7):2410–2419
13. Narayanasamy R, Padmanabhan P (2009) Application of response surface methodology for predicting bend force during air bending process in interstitial free steel sheet. Int J Adv Manuf Technol 44: 38–48
14. Yu HY (2009) Variation of elastic modulus during plastic deformation and its influence on springback. Mater Des 30:846–850
15. Ozturk F, Ece RE, Polat N, Koksal A (2010) Effect of warm temperature on springback compensation of titanium sheet. Mater Manuf Process 23(9):1021–1024
16. Chatti S, Hermi N (2011) The effect of non-linear recovery on springback prediction. Comput Struct 89(13–14):1367–1377
17. Baseri H, Bakhshi-Jooybari M, Rahmani B (2011) Modeling of spring-back in V-die bending process by using fuzzy learning back-propagation algorithm. Expert Syst Appl 38(7):8894–8900
18. Chen CC, Jiang CP (2011) Grain size effect in the micro-V-bending process of thin metal sheets. Mater Manuf Process 26(1):78–83
19. Lee JY, Lee JW, Lee MG, Barlat F (2012) An application of homogeneous anisotropic hardening to springback prediction in pre-strained U-draw/bending. Int J Solids Struct 49(25):3562–3572
20. Jiang CP, Chen CC (2012) Grain size effect on the springback behavior of the micro tube in the press bending process. Mater Manuf Process 27(5):512–518
21. Fu ZM (2012) Numerical simulation of springback in air-bending forming of sheet metal. Appl Mech Mater 121–126:3602–3606
22. Malikov V, Ossenbrink R, Viehweger B, Michailov V (2012) Experimental investigation and analytical calculation of the bending force for air bending of structured sheet metals. Adv Mater Res 418–420:1294–1300
23. Song Y, Yu Z (2013) Springback prediction in T-section beam bending process using neural networks and finite element method. Arch Civil Mech Eng 13(2):229–241
24. Leu DK (2013) Position deviation in V-die bending process with asymmetric bend length. Int J Adv Manuf Technol 64:93–103
25. Weinmann KJ, Shippell RJ (1978) Effect of tool and workpiece geometries upon bending forces and springback in 90 degree V-die bending of HSLA steel plate. In: Sixth North American Metal Working Research Conference Proceeding, pp 220–227
26. Ramezani M, Mohd Ripin Z, Ahmad R (2010) Modelling of kinetic friction in V-bending of ultra-high-strength steel sheets. Int J Adv Manuf Technol 46:101–110
27. Fu Z, Mo J (2010) Multiple-step incremental air-bending forming of high-strength sheet metal based on simulation analysis. Mater Manuf Process 25(8):808–816
28. Ramezani M, Mohd Ripin Z (2010) A friction model for dry contacts during metal-forming processes. Int J Adv Manuf Technol 51: 93–102
29. Fu Z, Mo J (2011) Springback prediction of high-strength sheet metal under air bending forming and tool design based on GA–BPNN. Int J Adv Manuf Technol 53(5–8):473–483
30. Kardes Sever N, Mete OH, Demiralp Y, Choi C, Altan T (2012) Springback prediction in bending of AHSS-DP 780. In: Proceedings of North American Manufacturing Research Institute/Society of Manufacturing Engineers, 40, pp 1–10
31. Leu DK (2015) Position deviation and springback in V-die bending process with asymmetric dies. Int J Adv Manuf Technol 79:1095–1108
32. Leu DK, Zhuang ZW (2016) Springback prediction of the vee bending process for high-strength steel sheets. J Mech Sci Technol 30(3):1077–1084
33. Morrison WB (1966) The effect of grain size on the stress-strain relationship in low-carbon steel. Trans Am Soc Met 59:824–846
34. Lopez Castro A, Durodola JF, Fellows NA (2009) A closed form solution for predicting springback in bending of beams including hardening effect. Adv Steel Constr 5(2):127–135
35. Zhang DJ, Cui ZS, Li YQ, Ruan XY (2006) The springback of wide metal sheet after large radius pure bending. Eng Mech 23(10):77–81 (in Chinese)